

# Photoelectron Spectroscopy of Cold Hydrated Sulfate Clusters, $\text{SO}_4^{2-}(\text{H}_2\text{O})_n$ ( $n = 4–7$ ): Temperature-Dependent Isomer Populations

Xue-Bin Wang,<sup>\*,†,‡</sup> Alina P. Sergeeva,<sup>§</sup> Jie Yang,<sup>†,‡</sup> Xiao-Peng Xing,<sup>†,‡</sup> Alexander I. Boldyrev,<sup>\*,§</sup> and Lai-Sheng Wang<sup>\*,†,‡</sup>

Department of Physics, Washington State University, 2710 University Drive, Richland, Washington 99354, Chemical & Materials Sciences Division, Pacific Northwest National Laboratory, MS K8-88, P.O. Box 999, Richland, Washington 99352, and Department of Chemistry and Biochemistry, Utah State University, Logan, Utah 84322

Received: January 23, 2009; Revised Manuscript Received: March 27, 2009

Sulfate is an important inorganic anion and its interactions with water are essential to understand its chemistry in aqueous solution. Studies of sulfate with well-controlled solvent numbers provide molecular-level information about the solute–solvent interactions and critical data to test theoretical methods for weakly bounded species. Here we report a low-temperature photoelectron spectroscopy study of hydrated sulfate clusters  $\text{SO}_4^{2-}(\text{H}_2\text{O})_n$  ( $n = 4–7$ ) at 12 K and ab initio studies to understand the structures and dynamics of these unique solvated systems. A significant increase of electron binding energies was observed for the 12 K spectra relative to those at room temperature, suggesting different structural isomers were populated as a function of temperature. Theoretical calculations revealed a competition between isomers with optimal water–solute and water–water interactions. The global minimum isomers all possess higher electron binding energies due to their optimal water-solute interactions, giving rise to the binding energy shift in the 12 K spectra, whereas many additional low-lying isomers with less optimal solvent–solute interactions were populated at room temperature, resulting in a shift to lower electron binding energies in the observed spectra. The current work demonstrates and confirms the complexity of the water-sulfate potential energy landscape and the importance of temperature control in studying the solvent–solute systems and in comparing calculations with experiment.

## 1. Introduction

Sulfate ( $\text{SO}_4^{2-}$ ) is a textbook inorganic polyanion and is ubiquitous in nature, such as in drinking water, soils, or atmospheric aerosols.<sup>1</sup> Sulfate particulates have been shown to act as nuclei for cloud formation<sup>2</sup> and hydrated sulfate minerals have been detected on the Martian surface.<sup>3</sup> Due to its compact and doubly charged nature, the interaction of sulfate with water is known to be strong and sulfate has a distinct position in the famous Hofmeister series.<sup>4</sup> However, an isolated sulfate dianion was shown to be unstable due to the strong intramolecular Coulomb repulsion of the two excess charges.<sup>5,6</sup> Blades and Kebarle<sup>6</sup> first observed hydrated sulfate clusters in the gas phase and performed collision-induced dissociation (CID) on selected  $\text{SO}_4^{2-}(\text{H}_2\text{O})_n$  clusters. Using photoelectron spectroscopy (PES) of size-selected anions, we showed previously that three water molecules are required to stabilize an isolated  $\text{SO}_4^{2-}$  in the gas phase<sup>7</sup> and further investigated its detailed solvation stabilization under room temperature (RT) conditions.<sup>8,9</sup> Since these initial studies, a series of recent experimental and theoretical investigations have been directed at the stability and solvation of the sulfate dianions,<sup>10–20</sup> and a diverse array of low-energy structures have been proposed for these species.

In particular, recent infrared (IR) spectroscopy studies have revealed valuable structural information about hydrated sulfate clusters.<sup>18,19</sup> However, due to the complexity of these systems,

a definite conclusion has not been reached for clusters with five or more waters. For example, in our earlier study,<sup>7</sup> we concluded that the global minimum of the hexamer,  $\text{SO}_4^{2-}(\text{H}_2\text{O})_6$ , possesses a  $C_3$  structure with three waters solvating  $\text{SO}_4^{2-}$  individually in a bidentate fashion and the other three waters forming a ring each with only one H-bond to the O atoms of  $\text{SO}_4^{2-}$ . This result has been confirmed later by Gao and Liu,<sup>16</sup> and Bush et al.<sup>19</sup> However, using IR spectroscopy of cold anions in a 17 K ion trap and theoretical calculations, Zhou et al.<sup>18</sup> concluded that  $\text{SO}_4^{2-}(\text{H}_2\text{O})_6$  has a  $T_d$  structure, in which each water molecule forms two H-bond with  $\text{SO}_4^{2-}$  along the six edges of the tetrahedral sulfate. In another IR study, Bush et al.<sup>19</sup> investigated  $\text{SO}_4^{2-}(\text{H}_2\text{O})_6$  in an ion cyclotron mass spectrometer at 130 K in the OH stretching region and suggested that many low-lying isomers were presented. The  $T_d$  structure for  $\text{SO}_4^{2-}(\text{H}_2\text{O})_6$  is the most symmetric and most tightly solvated structure with each O atom on  $\text{SO}_4^{2-}$  forming three H-bonds with water. It is the global minimum in the MP2 calculation in the study by Zhou et al.<sup>18</sup> However, this isomer is a relatively high-lying isomer both in our original study using DFT<sup>7–9</sup> and more recent DFT studies.<sup>15,16,19</sup> The difference between the studies by Zhou et al.<sup>18</sup> and Bush et al.<sup>19</sup> could be due to the different temperatures used in each experiment. The  $T_d$   $\text{SO}_4^{2-}(\text{H}_2\text{O})_6$  cluster should possess the highest electron binding energies compared to those lower symmetry structures that involve a less well solvated  $\text{SO}_4^{2-}$ . Thus, a temperature-dependent PES study of this cluster should be able to resolve this discrepancy.

We have recently developed a low-temperature ion trap PES apparatus coupled with an electrospray ionization source, which is aimed at performing PES for ultracold anions and investigating temperature-dependent phenomena.<sup>21,22</sup> We have demon-

\* Corresponding authors. E-mail: (X.-B.W.) xuebin.wang@pnl.gov; (A.I.B.) a.i.boldyrev@usu.edu; (L.S.W.) ls.wang@pnl.gov.

<sup>†</sup> Department of Physics, Washington State University.

<sup>‡</sup> Chemical & Materials Sciences Division, Pacific Northwest National Laboratory.

<sup>§</sup> Department of Chemistry and Biochemistry, Utah State University.

stressed the effects of temperature on conformation changes of a number of complex anions.<sup>21,23</sup> Here we further explore the hydrated sulfate systems,  $\text{SO}_4^{2-}(\text{H}_2\text{O})_n$  ( $n = 4-7$ ), under well-controlled temperature conditions using the low-temperature PES technique. Significant blue shifts of the electron binding energies were observed for these solvated clusters at 12 K relative to those at RT. With the aid of theoretical calculations, the electron binding energy shifts are understood as due to populations of different sets of isomers at different temperatures, directly revealing the existence of low-lying isomers for each cluster.

## 2. Experimental and Theoretical Methods

**2.1. Photoelectron Spectroscopy.** The low temperature PES apparatus, featuring an electrospray source, a low temperature ion trap, and a magnetic-bottle electron analyzer, has been described previously<sup>21,22</sup> and in more detail recently.<sup>24</sup> The solvated clusters,  $\text{SO}_4^{2-}(\text{H}_2\text{O})_n$ , were generated via electrospray of a 1 mM solution of tetrabutylammonium sulfate in a water/acetonitrile mixed solvent (1/3 volume ratio). The anions produced from the electrospray source were transported through two radio frequency quadrupole ion guides and a 90 degree ion bender followed by an octopole ion guide into a Paul trap, which is attached to the cold head of a close-cycle helium refrigerator (5–350 K). The temperature of the ion trap can be controlled between 10 to 350 K. Trapped ions were collisionally cooled by ~0.1 mTorr helium background gas containing 20% H<sub>2</sub> for experiments above 25 K. When the temperature is reduced to below 20 K, condensation of H<sub>2</sub> molecules on hydrated sulfate clusters has been observed,<sup>24,25</sup> and thus pure helium background gas was used instead. Ions were stored and cooled for 0.1 s in the Paul trap before being pulsed out into the extraction zone of a time-of-flight mass spectrometer at a 10 Hz repetition rate. Each hydrated sulfate cluster was mass-selected and decelerated before being intercepted by a detachment laser beam. We have studied the  $\text{SO}_4^{2-}(\text{H}_2\text{O})_n$  systems previously at several photon energies and a wide size range using our room temperature apparatus.<sup>7–9</sup> In the current study, we focus on the temperature effects in a limited size-range for  $n = 4-7$ , at both 266 nm (4.661 eV) from a Nd:YAG laser and 193 nm (6.424 eV) from an ArF excimer laser, as displayed in Figures 1–3. Photoelectrons were analyzed by a magnetic-bottle time-of-flight analyzer and were calibrated by the known spectra of I<sup>-</sup> and ClO<sub>2</sub><sup>-</sup>. The electron kinetic energy resolution of our PES spectrometer was  $\Delta E/E \sim 2\%$  or 20 meV for 1 eV electrons.

**2.2. Theoretical Methods.** Theoretical calculations were performed to sort out the low-lying isomers for  $\text{SO}_4^{2-}(\text{H}_2\text{O})_n$  ( $n = 4-7$ ) and to obtain theoretical vertical detachment energies (VDEs) to compare with the experimental data. Initial structures were based on those previously reported.<sup>15,16,18–20</sup> We reoptimized all the geometries of  $\text{SO}_4^{2-}(\text{H}_2\text{O})_n$  ( $n = 4-7$ ) and calculated frequencies using the hybrid DFT method known in the literature as B3LYP<sup>26–28</sup> with augmented correlation-consistent polarized double- $\zeta$  valence basis set (aug-cc-pVDZ).<sup>29</sup> All energy values of  $\text{SO}_4^{2-}(\text{H}_2\text{O})_n$  ( $n = 4-7$ ) clusters at B3LYP/aug-cc-pVDZ were corrected for zero-point vibrational energy (ZPE). We then performed single point calculations for all  $\text{SO}_4^{2-}(\text{H}_2\text{O})_n$  ( $n = 4-7$ ) isomers using the coupled-cluster method with single, double, and noniterative triple excitations [CCSD(T)]<sup>30–35</sup> based on the RHF formalism with the polarized split-valence basis sets (6-311++G\*\*)<sup>35–37</sup> at the optimized B3LYP/aug-cc-pVDZ geometries corrected for ZPE at the B3LYP/aug-cc-pVDZ level of theory. We arranged all the structures of  $\text{SO}_4^{2-}(\text{H}_2\text{O})_n$  ( $n = 4-7$ ) according to the relative energies obtained at the CCSD(T)/6-311++G\*\*//B3LYP/aug-

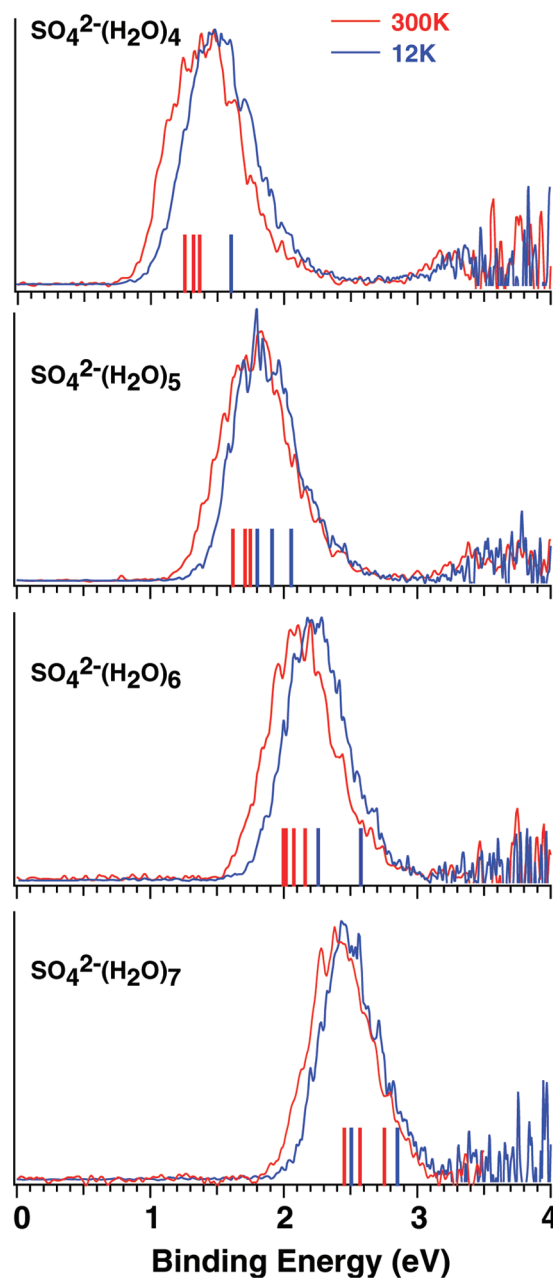


**Figure 1.** Photoelectron spectra of  $\text{SO}_4^{2-}(\text{H}_2\text{O})_n$  ( $n = 4-7$ ) at 266 nm (4.661 eV) at 12 K (blue) and at room temperature (red, data from ref 9). The vertical bars represent the calculated vertical detachment energies for the low-lying isomers. The blue bars indicate those from the global minimum isomers mainly populated at 12 K, while the red bars indicate additional isomers populated at room temperature.

cc-pVDZ + ZPE/B3LYP/aug-cc-pVDZ level of theory, as shown in Figures 4–7, respectively. Geometries and harmonic frequencies for the  $\text{SO}_4^{2-}(\text{H}_2\text{O})_6$  isomers were also calculated at the second order Moller–Plesset perturbation theory (MP2)<sup>36,37</sup> with the TZVP+ basis set derived from the DFT-optimized TZVP basis set<sup>38</sup> by addition of a diffuse *s* function to each H atom (exponent = 0.0457), and diffuse *s* and *p* functions to O and S atoms (exponents 0.0814 and 0.0481 on O, 0.0509 and 0.0342 on S). Our extensive studies show that the qualities of the TZVP+ and 6-311++G\*\* basis sets are comparable. Relative energies at MP2/TZVP+ corrected for ZPE at MP2/TZVP+ have been calculated for the hexamer only and are given in brackets in Figure 6. In the current work, we did not take into account the entropy effects, because our relative energies even at the CCSD(T)/6-311++G\*\*//B3LYP/aug-cc-pVDZ level

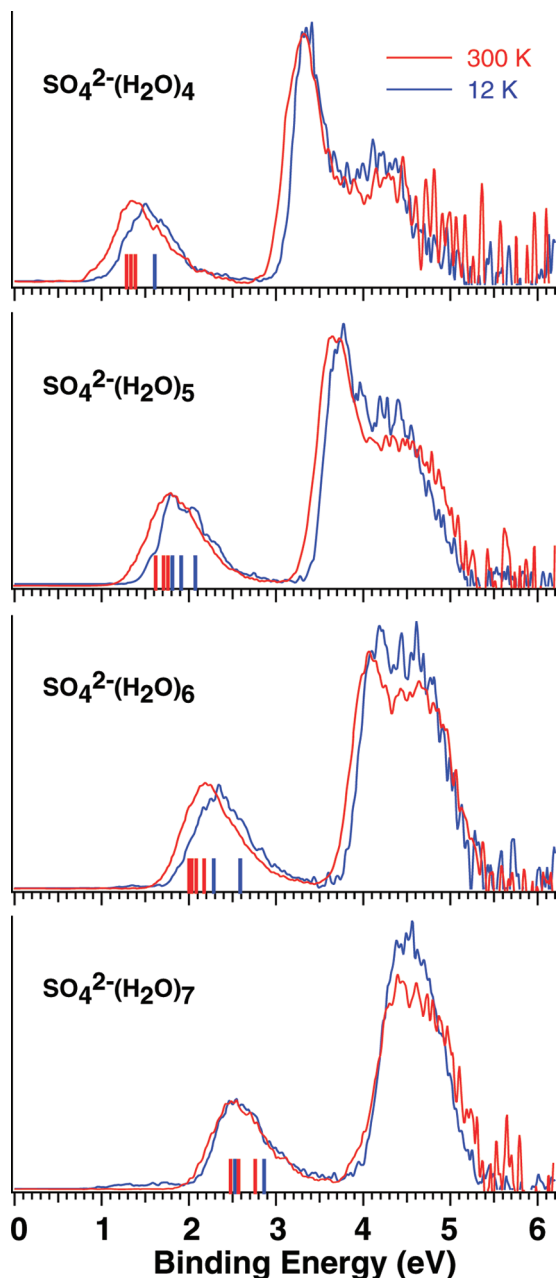


**Figure 2.** Photoelectron spectra of  $\text{SO}_4^{2-}(\text{H}_2\text{O})_n$  ( $n = 4–7$ ) at 193 nm (6.424 eV) at 12 K (blue) and at room temperature (red, data from ref 9). The solid bars are the same as in Figure 1.

of theory were not accurate enough to worry about these small corrections at such low temperature. We relied more on the calculated VDEs to explain which structures are responsible for the blue shift in the experimental PES of  $\text{SO}_4^{2-}(\text{H}_2\text{O})_n$  ( $n = 4–7$ ).

The first VDE for all species (Figures 4–7) was calculated at UB3LYP/6-311++G(2df,2pd)//B3LYP/aug-cc-pVDZ level of theory as the lowest transition from the optimized closed shell  $\text{SO}_4^{2-}(\text{H}_2\text{O})_n$  species to the doublet state of the  $\text{SO}_4^-(\text{H}_2\text{O})_n$  monoanion at the frozen geometry of the doubly charged species. Molecular orbital visualization was performed to elucidate which molecular orbitals the detachment channels occur from.

The B3LYP, MP2, and CCSD(T) calculations were performed using the Gaussian 03 program.<sup>39</sup> Molecular structure visualization was done using the MOLDEN 3.4 program.<sup>40</sup>

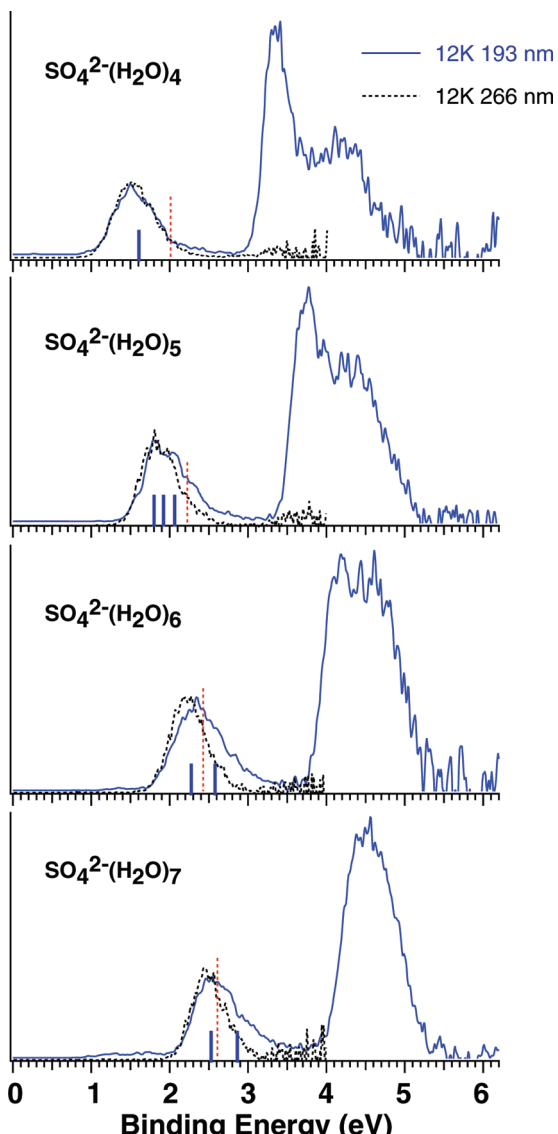


**Figure 3.** 12 K photoelectron spectra of  $\text{SO}_4^{2-}(\text{H}_2\text{O})_n$  ( $n = 4–7$ ) at 266 nm (black dashed) compared with those at 193 nm (solid blue), showing the effect of the repulsive Coulomb barrier on the 266 nm spectra. The solid vertical bars are the same as in Figures 1 and 2, representing the calculated vertical detachment energies for the global minimum isomers observed at 12 K. The dashed lines indicate the RCB cutoff positions at 266 nm.

### 3. Experimental Results: Low-Temperature Photoelectron Spectra of $\text{SO}_4^{2-}(\text{H}_2\text{O})_n$ ( $n = 4–7$ )

Figures 1 and 2 show the 266 and 193 nm spectra of  $\text{SO}_4^{2-}(\text{H}_2\text{O})_n$  ( $n = 4–7$ ), respectively, at 12 K (blue) compared to that at room temperature (red) reported previously in ref 9. The 193 nm spectra display two well-separated bands, one at lower electron binding energies and a broader feature at higher electron binding energies. These features are due to photoemission from the solute  $\text{SO}_4^{2-}$ , as discussed in detail in our previous RT studies.<sup>7–9</sup> The width of the features reflects the significant structural changes between the initial dianion and the final singly charged anion. Only the first band was observed in each case at 266 nm because of the repulsive Coulomb barrier (RCB), which prevents slow electrons from being emitted and is unique to PES of multiply charged anions.<sup>41–43</sup> The 12 K spectra are similar to the RT spectra, except a slight systematic shift toward higher binding energies (the shifts are due to the temperature effect because the two apparatuses were well calibrated). The

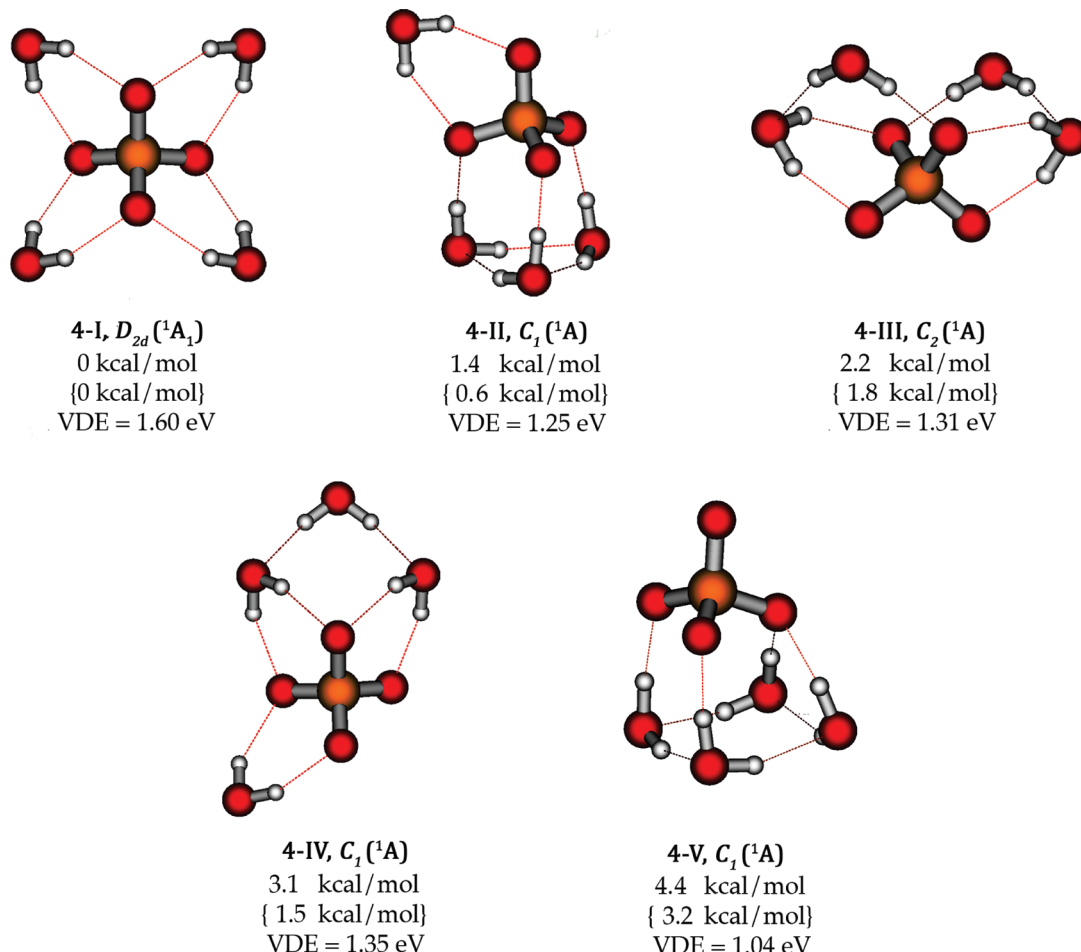


**Figure 4.** Optimized structures (at B3LYP/aug-cc-pVDZ), relative energies at CCSD(T)/6-311 ++G\*\*//B3LYP/aug-cc-pVDZ + ZPE//B3LYP/aug-cc-pVDZ and at B3LYP/aug-cc-pVDZ + ZPE//B3LYP/aug-cc-pVDZ (squiggle brackets), and the first VDEs (at B3LYP/6-311++ G(2df,2pd)//B3LYP/aug-cc-pVDZ) for the low-lying energy isomers of  $\text{SO}_4^{2-}(\text{H}_2\text{O})_n$ .

adiabatic detachment energy (ADE), measured from the threshold of the ground-state band, and the VDE, measured from the peak top from the 12 K spectra, are compared with those from the RT spectra in Table 1. The shift of VDE is size-dependent, ranging from 0.19 eV for  $n = 4$  to 0.10 eV for  $n = 7$ .

As shown previously,<sup>9</sup> the RCB in the  $\text{SO}_4^{2-}(\text{H}_2\text{O})_n$  solvated clusters is quite large, which not only cuts off the higher binding energy band in the 266 nm spectra (Figure 1), but also affect the ground-state band. This is shown more clearly in Figure 3, where the low temperature spectra at 266 and 193 nm are compared. The estimated RCB height from our previous study<sup>9</sup> is marked in each spectrum as a vertical dash line. Clearly, the RCB does not affect the 266 nm spectrum for  $n = 4$ , but it cuts off the higher binding energy part for  $n = 5-7$ .

Cold anions eliminate vibrational hot bands and are expected to result in sharper and better resolved PES spectra. However, the dominating effect for  $\text{SO}_4^{2-}(\text{H}_2\text{O})_n$  at low temperature is a spectral shift to higher binding energies, rather than a spectral sharpening. Similar temperature-dependent spectral shifts have been observed in a series of  $\text{CH}_3(\text{CH}_2)_n\text{CO}_2^-$  anions for  $n > 4$  previously.<sup>21</sup> These anions are linear at RT, but become cyclic at low temperatures due to the formation of a weak C-H $\cdots$ O hydrogen bond, which provides an extra stabilization to the electron binding energies of the carboxylate end group. The current observation of the spectral shift in  $\text{SO}_4^{2-}(\text{H}_2\text{O})_n$  suggests that different isomers (minima) maybe populated at different temperatures for these solvated clusters. It also indicates that transformation between isomers is facile, so no local minima

are trapped at the lowest temperatures. It is not surprising because of the floppy potential energy surfaces for these systems, albeit the exact barrier heights are unknown.<sup>16</sup> Since the electron binding energies are directly related to the solute–solvent interactions, the spectral shift implies that structures with stronger solute–solvent interactions are observed at low temperatures because these types of clusters are expected to possess higher electron binding energies.

#### 4. Theoretical Results: Low-Lying Isomers and Vertical Detachment Energies

The structures of  $\text{SO}_4^{2-}(\text{H}_2\text{O})_n$  have been calculated in several recent studies.<sup>15,16,18–20</sup> In particular, Gao and Liu<sup>15,16</sup> performed calculations for a wide size range using simulated annealing and DFT methods. To understand the temperature-dependent spectral shifts, we further reoptimized the geometries of  $\text{SO}_4^{2-}(\text{H}_2\text{O})_n$  ( $n = 4-7$ ) at B3LYP/aug-cc-pVDZ [in case of  $\text{SO}_4^{2-}(\text{H}_2\text{O})_6$ , also at MP2/TZVP+] and computed the VDEs for all the low-lying isomers. Since the relevant low-lying structures are all within only 2 to 4 kcal/mol for  $\text{SO}_4^{2-}(\text{H}_2\text{O})_n$  ( $n = 4-7$ ) at the B3LYP/aug-cc-pVDZ level of theory, we decided to perform CCSD(T)/6-311++G\*\* single point calculations at the optimized B3LYP/aug-cc-pVDZ geometries to see whether we could obtain better energetic information for the global minimum structures. Even though we call the lowest structures of  $\text{SO}_4^{2-}(\text{H}_2\text{O})_n$  ( $n = 4-7$ ) obtained at CCSD(T)/6-311++G\*\*//B3LYP/aug-cc-pVDZ to be the global minima, one

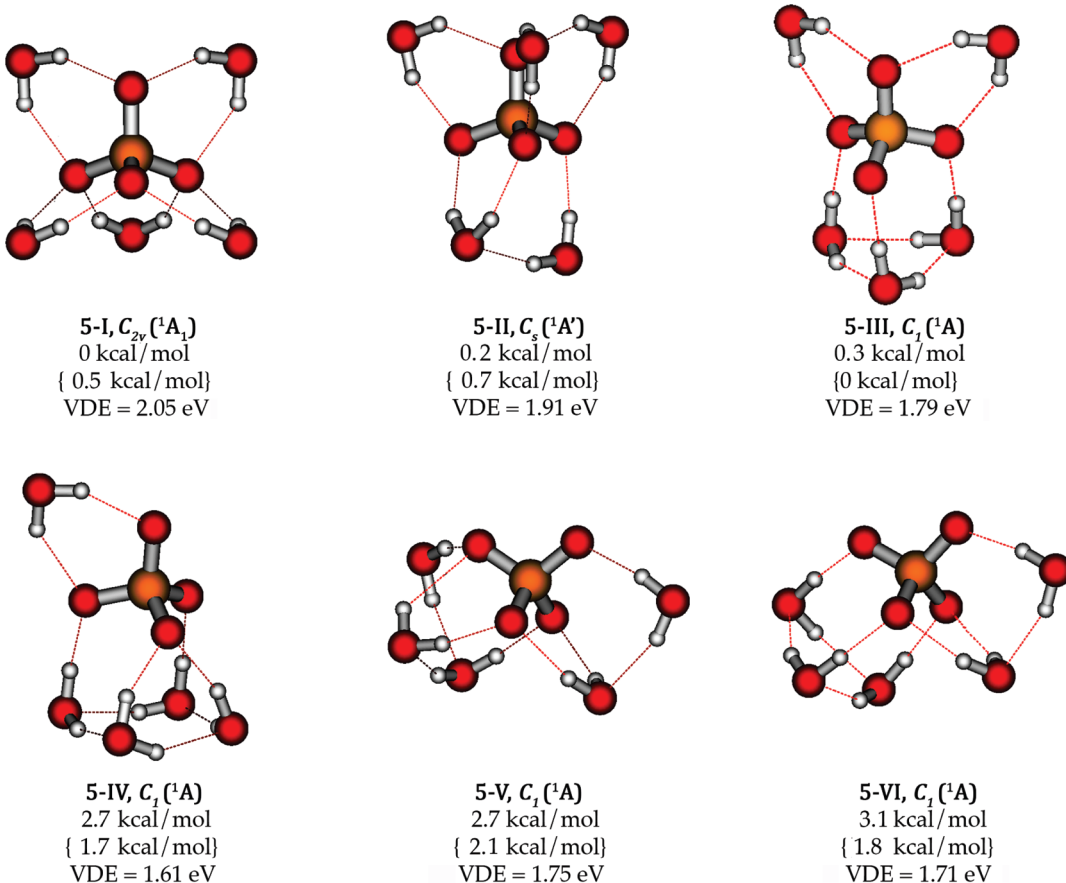


**Figure 5.** Optimized structures (at B3LYP/aug-cc-pVDZ), relative energies at CCSD(T)/6-311 ++G\*\*//B3LYP/aug-cc-pVDZ + ZPE//B3LYP/aug-cc-pVDZ and at B3LYP/aug-cc-pVDZ + ZPE//B3LYP/aug-cc-pVDZ (squiggle brackets), and the first VDEs (at B3LYP/6-311++ G(2df,2pd)//B3LYP/aug-cc-pVDZ) for the low-lying energy isomers of  $\text{SO}_4^{2-}(\text{H}_2\text{O})_5$ .

should be cautioned that the accuracy of any method [including CCSD(T)] is not enough in the current cases to make a proper ordering of the isomers because of their relatively small energy differences, as shown in Figures 4–7. The VDEs are presented as vertical solid bars in Figures 4–7. The computed VDEs can be the only criteria for explaining the experimental PES spectra.

In the following discussion, the relative energies all refer to the CCSD(T)/6-311++G\*\*// B3LYP/ aug-cc-pVDZ + ZPE// B3LYP/aug-cc-pVDZ level of theory and the VDEs refer to the B3LYP/ 6-311++G(2df,2pd)//B3LYP/aug-cc-pVDZ level of theory, unless noted otherwise.

**4.1.  $\text{SO}_4^{2-}(\text{H}_2\text{O})_4$ .** Five isomers (labeled as 4-I to 4-V) are found for  $n = 4$ , as shown in Figure 4. The global minimum structure 4-I is the same as was originally suggested<sup>7</sup> and confirmed recently.<sup>16,18</sup> In this structure, each of the four waters forms two hydrogen bonds with the oxygen atoms of  $\text{SO}_4^{2-}$  in a bidentate fashion, optimizing the solvent–solute interactions without any solvent–solvent interactions. A low-lying isomer 4-II is found to be only 1.4 kcal/mol higher, in which three of the waters form a ring. It appears that the solvent–solvent interactions are competing with the solvent–solute interactions even at  $n = 4$ . Three other isomers (4-III, 4-IV, and 4-V) with higher energies of 2.2, 3.1, and 4.4 kcal/mol, respectively, are also found, which all involve water–water interactions. Not surprisingly, the global minimum 4-I yields the highest VDE at 1.60 eV due to the optimal solute–solvent interactions. All the other low-lying isomers yield lower VDEs, with isomer 4-V giving the lowest VDE at 1.04 eV because in this isomer the  $\text{SO}_4^{2-}$  solute is least solvated.

**4.2.  $\text{SO}_4^{2-}(\text{H}_2\text{O})_5$ .** The low-lying isomers for  $n = 5$  are shown in Figure 5. Isomers 5-I and 5-II were suggested

previously as global minimum structures<sup>7,16,18,20</sup> and they differ in energy by only 0.2 kcal/mol in the current calculations. A new isomer 5-III is found to be higher in energy only by 0.3 kcal/mol. Thus, these three isomers should be considered to be competing for the global minimum. In isomer 5-III, two of the five waters form hydrogen bonds with oxygen atoms of  $\text{SO}_4^{2-}$  in a bidentate fashion and the other three waters form a ring like in isomer 4-II (Figure 4). Clearly, solvent–solvent interactions start to be more competitive in  $\text{SO}_4^{2-}(\text{H}_2\text{O})_5$ . Only in isomer 5-I do all five waters bind to the solute in bidentate fashion without any solvent–solvent interactions. The other three isomers (5-IV, 5-V, 5-VI), which involve more extensive solvent–solvent interactions, are higher in energy by 2.7, 2.7, and 3.1 kcal/mol, respectively.

Again, the global minimum 5-I structure with optimal solute–solvent interactions yields the highest VDE at 2.05 eV. The nearly degenerate 5-II and 5-III isomers give slightly lower VDEs of 1.91 and 1.79 eV, respectively. Isomers 5-IV, 5-V and 5-VI all give lower VDEs at 1.61, 1.75, and 1.71 eV, respectively.

**4.3.  $\text{SO}_4^{2-}(\text{H}_2\text{O})_6$ .** The low-lying structures of  $\text{SO}_4^{2-}(\text{H}_2\text{O})_6$  studied in this work are presented in Figure 6. We optimized geometries and calculated harmonic frequencies at two levels of theory: B3LYP/aug-cc-pVDZ and MP2/TZVP+. We also performed single point CCSD(T)/6-311++G\*\* calculations at the optimized B3LYP/aug-cc-pVDZ geometries to show how the relative energies depend on the theoretical methods. The relative energies at the three levels of theory are given in Figure 6, B3LYP/aug-cc-pVDZ+ZPE//B3LYP/aug-cc-pVDZ in squiggle brackets and MP2/TZVP+//MP2/TZVP+ + ZPE//MP2/TZVP+ in brackets.

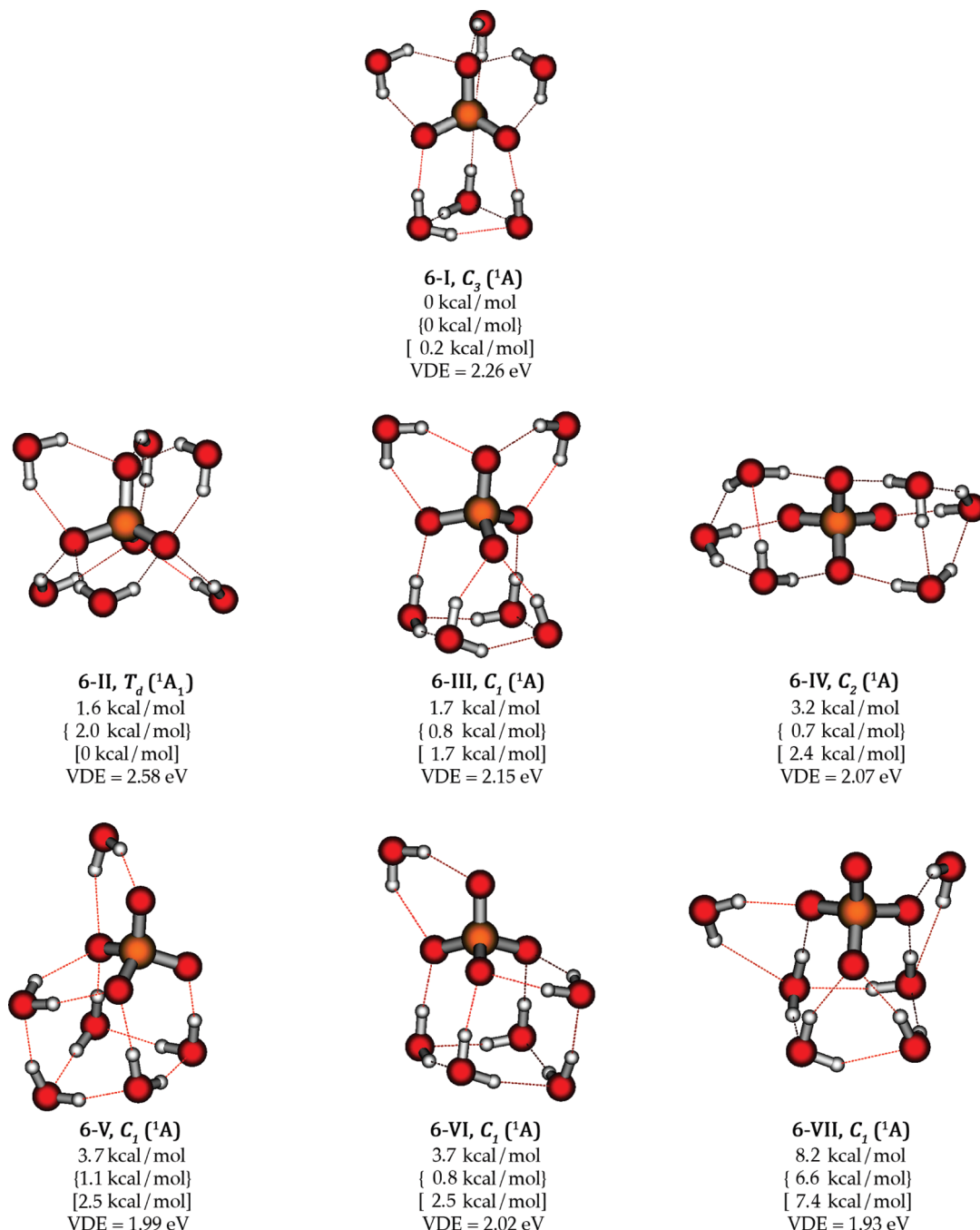


**Figure 6.** Optimized structures (at B3LYP/aug-cc-pVDZ), relative energies at CCSD(T)/6-311 ++G\*\*//B3LYP/aug-cc-pVDZ + ZPE//B3LYP/aug-cc-pVDZ, at B3LYP/aug-cc-pVDZ + ZPE/B3LYP/aug-cc-pVDZ (squiggle brackets), at MP2/TZVP+//MP2/TZVP+ + ZPE/MP2/TZVP+ (square brackets), and the first VDEs (at B3LYP/6-311++ G(2df,2pd)//B3LYP/aug-cc-pVDZ) for the low-lying energy isomers of  $\text{SO}_4^{2-}(\text{H}_2\text{O})_6$ .

Both isomers 6-I and 6-II have been reported previously as the global minimum structure for  $\text{SO}_4^{2-}(\text{H}_2\text{O})_6$ . At the B3LYP/aug-cc-pVDZ level of theory, the  $C_3$  (6-I) structure is the most stable one in agreement with our original work,<sup>7</sup> with four close-lying isomers (6-III, 6-IV, 6-V, and 6-VI) within about 1 kcal/mol. Two other isomers (6-II) and (6-VII) are lying higher by 2.0 and 6.6 kcal/mol, respectively. However, at the MP2/TZVP+ level of theory, we found that the most stable structure is the  $T_d$  isomer 6-II, in agreement with Zhou et al.<sup>18</sup> At this level of theory, the  $C_3$  isomer 6-I is almost isoenergetic with the  $T_d$  isomer only 0.2 kcal/mol higher in energy, but all other isomers, 6-III, 6-IV, 6-V, 6-VI, and 6-VII, are substantially higher by 1.7, 2.4, 2.5, 2.5, and 7.4 kcal/mol, respectively. At the CCSD(T)/6-311++G\*\* level of theory, the  $C_3$  isomer 6-I is

again the most stable one in agreement with the B3LYP/aug-cc-pVDZ results, whereas the  $T_d$  isomer 6-II becomes the second isomer higher in energy by 1.6 kcal/mol. The other isomers, 6-III, 6-IV, 6-V, and 6-VI, are higher in energy by 1.7, 3.2, 3.7, and 3.7 kcal/mol, respectively. These results show that the potential energy surfaces of the hydrated  $\text{SO}_4^{2-}$  clusters are quite complex with many local minima, and it is quite challenging to predict computationally with certainty the global minimum structure.

The global minimum 6-I structure gives a VDE of 2.26 eV, whereas the  $T_d$  6-II isomer gives a very high VDE of 2.58 eV, as expected. In all the other isomers, the  $\text{SO}_4^{2-}$  solute is less well solvated and their VDEs are lower, ranging from 1.93 to 2.15 eV, as given in Figure 6.

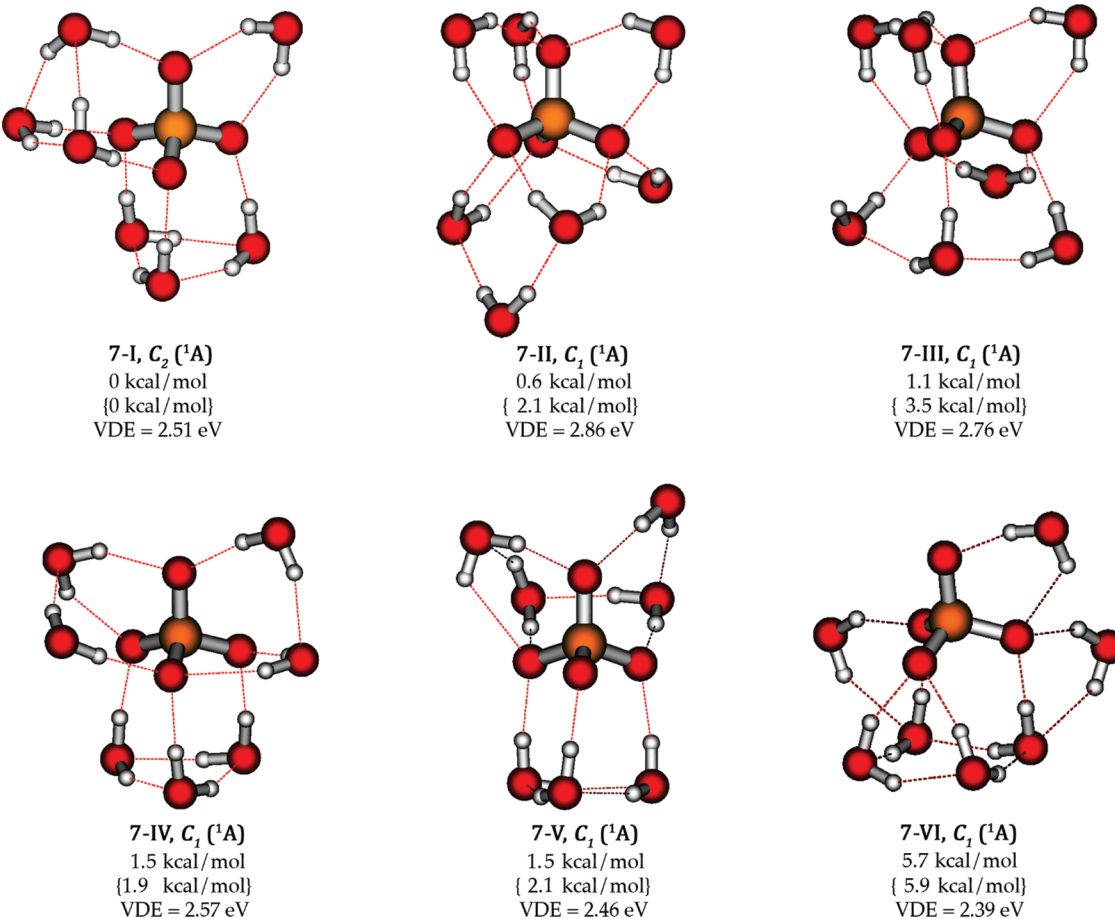


**Figure 7.** Optimized structures (at B3LYP/aug-cc-pVDZ), relative energies at CCSD(T)/6-311 ++G\*\*//B3LYP/aug-cc-pVDZ + ZPE//B3LYP/aug-cc-pVDZ and at B3LYP/aug-cc-pVDZ + ZPE//B3LYP/aug-cc-pVDZ (squiggle brackets), and the first VDEs (at B3LYP/6-311++ G(2df,2pd)//B3LYP/aug-cc-pVDZ) for the low-lying energy isomers of  $\text{SO}_4^{2-}(\text{H}_2\text{O})_n$ .

**TABLE 1: Experimental Adiabatic (ADE), Vertical (VDE) Electron Detachment Energies, and the VDE Increase ( $\Delta$ VDE) in the 12 K Spectra Relative to Those at Room Temperature (RT) for  $\text{SO}_4^{2-}(\text{H}_2\text{O})_n$  ( $n = 4-7$ )<sup>a</sup>**

$n$	ADE <sup>b</sup>		VDE <sup>c</sup>		$\Delta$ VDE exp <sup>d</sup>
	RT	12 K	RT	12 K	
4	0.92(8)	1.15(8)	1.33(10)	1.52(10)	0.19 (5)
5	1.36(8)	1.48(8)	1.70(10)	1.80(10)	0.10 (5)
6	1.71(8)	1.88(8)	2.10(10)	2.25(10)	0.15 (5)
7	2.08(8)	2.15(8)	2.40(10)	2.50(10)	0.10 (5)

<sup>a</sup> All energies are in eV. Numbers in parentheses represent experimental uncertainties in the last digits. The room temperature data are from ref.<sup>9</sup> <sup>b</sup> The ADE was estimated by drawing a straight line at the leading edge of the 266 nm spectral band at 12 K and then adding the instrumental resolution to the intersection with the binding energy axis. The uncertainty is largely due to the fact that the rising edge is not perfectly smooth, and the 80 meV error bar is estimated from measuring many spectra. <sup>c</sup> Measured from the maximum of the band from the 266 nm spectra at 12 K. Due to the broadness of the feature, the exact maximum position cannot be accurately determined, resulting in 100 meV uncertainty. <sup>d</sup>  $\Delta$ VDE with smaller uncertainty because the spectral shift can be measured more accurately by canceling systematic errors.

**4.4.  $\text{SO}_4^{2-}(\text{H}_2\text{O})_7$ .** Six low-lying isomers were found for  $\text{SO}_4^{2-}(\text{H}_2\text{O})_7$ , as presented in Figure 7. Isomer 7-I, which contains two three-water rings, is the global minimum. Isomer 7-II, which is built from the  $T_d$   $\text{SO}_4^{2-}(\text{H}_2\text{O})_6$ , is almost degenerate with 7-I, only 0.6 kcal/mol higher in energy. These two structures are consistent with those obtained by Zhou et

al.<sup>18</sup> Three more low-lying isomers (7-III, 7-IV, 7-V) were found to be within 1.5 kcal/mol above the global minimum. Isomer 7-VI was found to be 5.7 kcal/mol higher in energy.

Isomer 7-I gives a VDE of 2.51 eV, whereas isomer 7-II yields the highest VDE at 2.86 eV because  $\text{SO}_4^{2-}$  is best solvated in this isomer with each O atom forming three H-bonds with water similar to the  $T_d$  isomer for  $\text{SO}_4^{2-}(\text{H}_2\text{O})_6$ . Isomers 7-III, 7-IV, and 7-V give VDEs of 2.76, 2.57, and 2.46 eV, respectively. Isomer 7-VI yields the lowest VDE at 2.39 eV because  $\text{SO}_4^{2-}$  is not well solvated in this isomer.

We analyzed the molecular orbitals and found that the first VDE for all the  $\text{SO}_4^{2-}(\text{H}_2\text{O})_n$  ( $n = 4-7$ ) clusters indeed comes from an electron detachment from the  $\text{SO}_4^{2-}$  solute. The second VDEs in all the species stand for electron detachment from the molecular orbital with contribution from both  $\text{SO}_4^{2-}$  solute and  $\text{H}_2\text{O}$  solvent. Electron detachments from the solvent-only orbitals appear first at the forth VDE in all the  $\text{SO}_4^{2-}(\text{H}_2\text{O})_n$  ( $n = 4-7$ ) clusters except for the 4-V and 6-III isomers. In the 4-V and 6-III isomers, the fifth VDE comes from an electron detachment from the solvent. These results confirm our previous assignments for the photodetachment features for the  $\text{SO}_4^{2-}(\text{H}_2\text{O})_n$  solvated clusters at room temperature (RT).<sup>7-9</sup>

## 5. Discussions

The electron binding energies of the hydrated clusters directly reflect how  $\text{SO}_4^{2-}$  is solvated by the  $\text{H}_2\text{O}$  molecules. It is expected that structures with optimal dianion-water interactions should give higher electron binding energies, whereas structures

with less well-solvated  $\text{SO}_4^{2-}$  should yield lower electron binding energies. Therefore, comparison of the calculated electron binding energies with the temperature-dependent PES spectra should provide information about the isomers populated at different temperatures and help identify the global minimum structures. The calculated first VDEs for the low-lying isomers of  $\text{SO}_4^{2-}(\text{H}_2\text{O})_n$  ( $n = 4-7$ ) are given as solid bars in Figures 1 and 2.

**5.1.  $\text{SO}_4^{2-}(\text{H}_2\text{O})_4$ .** All previous calculations predicted that isomer 4-I as the global minimum,<sup>7,16,18,20</sup> while other isomers with water–water H-bonding are considerably higher in energy. Zhou et al.<sup>18</sup> reported the IR spectrum of this cluster at 17 K in the spectral region of water bending, and  $\text{SO}_2$  asymmetric stretching and bending. The observed IR spectrum agreed well with the simulated spectrum based on isomer 4-I, confirming the global minimum for  $n = 4$ . Our low temperature PES spectra showed an increase of VDE by about 0.19 eV relative to that at RT. Indeed, the current calculations predict that the global minimum isomer 4-I has the highest VDE at 1.60 eV among all the low-lying isomers, in excellent agreement with the low temperature PES spectra (Figure 1, blue bar).

Several low-lying isomers with water–water H-bonding are found for  $\text{SO}_4^{2-}(\text{H}_2\text{O})_4$  (Figure 4). In particular, isomer 4-II is only 1.4 kcal/mol higher in energy. A similar low-lying isomer was previously reported by Gao and Liu.<sup>16</sup> This isomer is expected to be populated at RT. Because  $\text{SO}_4^{2-}$  is not well solvated in this isomer, its computed first VDE is significantly lower than the global minimum structure, in good agreement with the PES spectra at RT. Although isomers 4-III and 4-IV are higher in energy by 2.2 and 3.1 kcal/mol, respectively, their computed first VDEs (1.31 and 1.35 eV), are also in good agreement with the RT PES spectra. Thus, they might also be populated at RT. However, isomer 4-V is much higher in energy by 4.4 kcal/mol; its calculated first VDE at 1.04 is also too low, inconsistent with the RT spectra, and its population at RT can be safely ruled out. Thus, we can conclude unambiguously that isomer 4-I is indeed the global minimum and is the dominant species at 12 K, consistent with the previous IR study,<sup>18</sup> whereas at RT both isomers 4-I and 4-II, and possibly 4-III and 4-IV, are also populated, giving rise to the apparent lower binding energies in the PES spectra.

**5.2.  $\text{SO}_4^{2-}(\text{H}_2\text{O})_5$ .** The first three isomers (5-I, 5-II, and 5-III) of  $\text{SO}_4^{2-}(\text{H}_2\text{O})_5$  are within 0.3 kcal/mol of each other (Figure 5) and their calculated VDEs (2.05, 1.91, and 1.79 eV, respectively) are all within the bandwidth of the PES spectra at 12 K. Thus, they could be all populated even at 12 K. Although Zhou et al.<sup>18</sup> achieved good agreement between the simulated IR spectrum of isomer 5-I with the experimental spectrum, later calculations showed that isomer 5-II could also produce a very similar IR spectrum.<sup>20</sup> Indeed, different global minima have been obtained using different methods, but the energy differences are all small among these three isomers.<sup>7,16,19,20</sup> Isomers 5-IV, 5-V, and 5-VI are significantly higher in energy and their calculated first VDEs are rather close to each other. Because  $\text{SO}_4^{2-}$  is clearly less well solvated in these isomers, their VDEs are lower (1.65, 1.75, and 1.71 eV, respectively) in agreement with the RT PES spectra, suggesting that besides 5-I, 5-II, and 5-III they were also populated significantly at RT.

**5.3.  $\text{SO}_4^{2-}(\text{H}_2\text{O})_6$ .** The global minimum of  $\text{SO}_4^{2-}(\text{H}_2\text{O})_6$  was initially reported to be the  $C_3$  isomer 6-I,<sup>7</sup> which was confirmed by further DFT calculations.<sup>16,19</sup> However, Zhou et al.<sup>18</sup> reported that the  $T_d$  isomer 6-II was the global minimum using MP2 calculations and showed that the simulated IR spectrum of the  $T_d$  isomer agreed with the experiment. Our current DFT

calculations at the B3LYP level also gave the  $C_3$  structure as the global minimum (Figure 6). We further carried our MP2 calculations for  $\text{SO}_4^{2-}(\text{H}_2\text{O})_6$  and confirmed the result of Zhou et al., but the  $C_3$  isomer is only 0.2 kcal/mol higher (Figure 6) at this level of theory, essentially isoenergetic with the  $T_d$  isomer. However, at our highest level of theory using CCSD(T), the  $C_3$  structure is shown indeed to be the global minimum, while the  $T_d$  isomer is 1.6 kcal/mol higher. Interestingly, even though Zhou et al. assigned the  $T_d$  structure to the observed IR spectrum of  $\text{SO}_4^{2-}(\text{H}_2\text{O})_6$ , their simulated IR spectrum for the  $C_3$  isomer is also in quite good agreement with the experimental spectrum if one takes into account the relative IR peak intensities.<sup>18</sup> We also found several other low-lying isomers, consistent with the reports by Gao and Liu<sup>16</sup> and Bush et al.<sup>19</sup> In particular, we found that isomer 6-III is quite close in energy to the  $T_d$  isomer only 1.7 kcal/mol above the global minimum. Three other isomers, 6-IV, 6-V, and 6-VI, are energetically low-lying isomers, but isomer 6-VII is much higher in energy and will not be considered further.

The calculated VDE for the  $C_3$  isomer 6-I at 2.26 eV is in excellent agreement with the PES spectrum at 12 K, whereas the VDE for the  $T_d$  structure 6-II at 2.58 eV is very high, lying at the high binding energy end of the 266 nm spectrum (Figure 1). However, as noted in Section 3, the 266 nm spectrum was affected by the RCB cutoff, as shown more clearly in Figure 3. The 193 nm spectrum at 12 K is indeed broader in the higher binding energy side, so we cannot completely rule out contributions to this part of the spectrum by the  $T_d$  isomer at 12 K. The calculated VDEs for isomers 6-III, 6-IV, 6-V, and 6-VI are clearly lower, all around 2 eV, which agree well with the RT PES spectra (Figure 1). Thus, at room temperature, the first six isomers should be populated. Interestingly, Bush et al. showed in their IR study in the OH stretching region that at least two isomers ( $C_3$  6-I and  $T_d$  6-II) or more structures are contributing to the observed spectrum even at 130 K.<sup>19</sup>

**5.4.  $\text{SO}_4^{2-}(\text{H}_2\text{O})_7$ .** Six low-lying minima are identified in the current study and displayed in Figure 7. Similar structures were reported by Gao and Liu<sup>16</sup> and Zhou et al.<sup>18</sup> The global minimum isomer 7-I gives a VDE of 2.51 eV, which is in good agreement with the 12 K PES spectrum (Figure 1). However, isomer II is nearly isoenergetic with 7-I and Zhou et al. suggested coexistence of these two isomers by comparing the observed IR spectrum with the simulated ones. Isomer 7-II is built upon isomer 6-II and has the highest VDE, which appears to disagree with the 266 nm PES spectrum at 12 K (Figure 1). Similar to the 266 nm spectrum of  $\text{SO}_4^{2-}(\text{H}_2\text{O})_6$ , there is also a cutoff by the RCB for  $\text{SO}_4^{2-}(\text{H}_2\text{O})_7$ , as shown in Figure 3, where the tail on the high binding energy side in the ground-state band agrees well with the VDE of isomer 7-II. Isomers 7-III, 7-IV, and 7-V are relatively low-lying and should be populated at RT. However, their calculated VDEs are not significantly lower than those of isomers 7-I and 7-II, consistent with the fact that the 12 K PES spectra of  $\text{SO}_4^{2-}(\text{H}_2\text{O})_7$  exhibited only a very small increase in electron binding energies (Figures 1 and 2).

**5.5. Structural Evolution in  $\text{SO}_4^{2-}(\text{H}_2\text{O})_n$  and Competition between Water– $\text{SO}_4^{2-}$  and Water–Water Interactions.** Because of the doubly charged nature of  $\text{SO}_4^{2-}$ , we expected that the solute–water interactions should dominate the solvated cluster structures in  $\text{SO}_4^{2-}(\text{H}_2\text{O})_n$ . This is indeed the case for  $n = 1-4$ , where each water forms two H-bonds with  $\text{SO}_4^{2-}$  without any water–water interactions.<sup>7</sup> However, starting at  $n = 5$ , the water–water interactions are competitive with water–solute interactions. Even though isomer 5-I, which has no water–water H-bond, is the global minimum, isomers 5-II

and 5-III with one and three water–water H-bonds, respectively, are almost isoenergetic to isomer 5-I (Figure 5). For  $n \geq 6$ , the global minima are basically dominated by structures with increasing degrees of water–water H-bonding. We note that the three-water ring bonded to one face of the  $\text{SO}_4^{2-}$  tetrahedron is a particularly favorable structural unit. Even for  $n = 4$ , the isomer 4-II, the closest-lying isomer above the global minimum, contains such a structural unit, whereas in  $n = 5$  the isomer containing a three-water ring (isomer 5-III) is already competing for the global minimum. In  $n = 6$ , the global minimum isomer 6-I contains a three-water ring: the water–water interactions entailed in the three-water ring and the water–solute interactions seem to achieve a good compromise to yield the interesting  $C_3$  global minimum, whereas the  $T_d$  isomer 6-II without any water–water H-bond is a low-lying isomer (Figure 6). In  $n = 7$ , the global minimum contains two three-water rings. The unique stability of the three-water ring would lead to a highly stable structure in  $n = 12$  with four such three-water rings bonded to the four faces of the  $\text{SO}_4^{2-}$  tetrahedron, which is indeed found to be the case in the previous IR studies by Zhou et al.<sup>12,18</sup>

H-bonding with negative charge centers is supposed to be stronger than water–water H-bonding. However, the two negative charges in  $\text{SO}_4^{2-}$  are delocalized on the four O centers, yielding on average  $-0.5$  charge per O atom. It seems that it is optimal for each  $\text{O}^{-0.5}$  center on  $\text{SO}_4^{2-}$  to form two H-bonds with water, which is achieved already in  $\text{SO}_4^{2-}(\text{H}_2\text{O})_4$  in isomer 4-I. Additional H-bond to the  $\text{O}^{-0.5}$  centers on  $\text{SO}_4^{2-}$  does not seem to be significantly advantageous energetically, making the water–water H-bonding competitive for  $n > 4$ .

**5.6. Temperature-Dependent Spectral Shifts and Conformation Changes.** The excellent agreement between the calculated VDEs for different low-lying isomers and the observed temperature-dependent PES spectra for  $\text{SO}_4^{2-}(\text{H}_2\text{O})_n$  ( $n = 4–7$ ) confirms unequivocally that different isomers were populated at different temperatures. This is a significant observation and it is unique to weakly bound systems. For strongly bound and rigid molecular species, cold anions result in better resolved PES spectra due to the elimination of hot band transitions.<sup>21–24,44–47</sup> However, for weakly bound systems with close-lying isomers, higher temperatures allow populations of slightly higher lying isomers. If these isomers have different electronic structures, totally different PES spectra can be observed as a function of temperature. In the current case, since the sulfate is the electron emission center regardless of the detailed solvated structures, spectral shifts are observed as a function of temperature due to the populations of different isomers. Such PES spectral shift has been observed previously in  $\text{CH}_3(\text{CH}_2)_n\text{CO}_2^-$  due to linear to cyclic conformation changes with decreasing temperature.<sup>21</sup> The current results demonstrate the importance of temperature control in the study of weakly bound clusters and reinforce the idea that cold ions are crucial in order to compare with theoretical calculations for the identification of global minima for these systems.

## 6. Conclusions

We report a low-temperature photoelectron spectroscopy study of  $\text{SO}_4^{2-}(\text{H}_2\text{O})_n$  ( $n = 4–7$ ) at 12 K, showing that the low-temperature PES spectra all display a shift to higher binding energies relative to the room temperature data. Theoretical calculations were carried out using both DFT method and *ab initio* methods at MP2 and CCSD(T) levels of theory, revealing a diverse array of low-lying isomers. The VDEs of the global minimum structures were shown to be higher because of the

favorable solute–solvent interactions, whereas higher energy isomers give rise to lower VDEs because of the less favorable solute–solvent interactions. Comparison between the calculated VDEs and the temperature-dependent PES data show that different isomers were probed experimentally at different temperatures. The low temperature data were mainly due to the global minimum isomers, whereas at room temperature many low-lying isomers were also populated. Competition between solvent–solute and solvent–solvent interactions is observed as a function of cluster size. While solvent–solute interactions dominate the structures for  $n$  up to 4, solvent–solvent interactions become competitive for  $n$  beyond 4. The current joint experimental and theoretical study on the hydrated sulfate clusters shows the importance to perform experiments at well-controlled temperatures for weakly bonded species in order to compare with calculations because of the presence of multiple low-lying isomers and their populations at high temperatures.

**Acknowledgment.** The experimental work was supported by the U.S. Department of Energy (DOE), Office of Basic Energy Sciences, Chemical Sciences Division and was performed at the EMSL, a national scientific user facility sponsored by DOE's Office of Biological and Environmental Research and located at Pacific Northwest National Laboratory, which is operated for DOE by Battelle. The theoretical work done at Utah State University was supported by the National Science Foundation (CHE-07148510). Computer time from the Center for High Performance Computing at Utah State University is gratefully acknowledged. The computational resource, the Uinta cluster supercomputer, was provided through the National Science Foundation under Grant CTS-0321170 with matching funds provided by Utah State University.

**Supporting Information Available:** Tables of total energies and Cartesian coordinates of  $\text{SO}_4^{2-}(\text{H}_2\text{O})_n$  ( $n = 4–7$ ) isomers optimized at B3LYP/aug-cc-pVQZ. This material is available free of charge via the Internet at <http://pubs.acs.org>.

## References and Notes

- (1) Ramanathan, V.; Crutzen, P. J.; Kiehl, J. T.; Rosenfeld, D. *Science* **2001**, 294, 2119.
- (2) Abbott, J. P. D.; Benz, S.; Cziczo, D. J.; Kanji, Z.; Lohmann, U.; Mohler, O. *Science* **2006**, 313, 1770.
- (3) Bibring, J. P.; et al. *Science* **2006**, 312, 400.
- (4) Zhang, Y.; Cremer, P. S. *Curr. Opin. Chem. Biol.* **2006**, 10, 658.
- (5) Boldyrev, A. I.; Simons, J. *J. Phys. Chem.* **1994**, 98, 2298.
- (6) Blades, A. T.; Kebarle, P. *J. Am. Chem. Soc.* **1994**, 116, 10761.
- (7) Wang, X. B.; Nicholas, J. B.; Wang, L. S. *J. Chem. Phys.* **2000**, 113, 10837.
- (8) Wang, X. B.; Yang, X.; Nicholas, J. B.; Wang, L. S. *Science* **2001**, 294, 1322.
- (9) Yang, X.; Wang, X. B.; Wang, L. S. *J. Phys. Chem. A* **2002**, 106, 7607.
- (10) Stefanovich, E.; Boldyrev, A. I.; Troung, T.; Simons, J. *J. Phys. Chem.* **1998**, 102, 4205.
- (11) Whitehead, A.; Barrios, R.; Simons, J. *J. Chem. Phys.* **2002**, 116, 2848.
- (12) Wong, R. L.; Williams, E. R. *J. Phys. Chem. A* **2003**, 107, 10976.
- (13) Zhan, C. G.; Zheng, F.; Dixon, D. A. *J. Chem. Phys.* **2003**, 119, 781.
- (14) Jungwirth, P.; Curtis, J. E.; Tobias, D. J. *Chem. Phys. Lett.* **2003**, 367, 704.
- (15) Gao, B.; Liu, Z. F. *J. Chem. Phys.* **2004**, 121, 8299.
- (16) Gao, B.; Liu, Z. F. *J. Chem. Phys.* **2005**, 123, 224302.
- (17) Blades, A. T.; Kebarle, P. *J. Phys. Chem. A* **2005**, 109, 8293.
- (18) Zhou, J.; Santambrogio, G.; Brümmer, M.; Moore, D. T.; Wöste, L.; Meijer, G.; Neumark, D. M.; Asmis, K. R. *J. Chem. Phys.* **2006**, 125, 111102.
- (19) Bush, M. F.; Saykally, R. J.; Williams, E. R. *J. Am. Chem. Soc.* **2007**, 129, 2220.
- (20) Miller, Y.; Chaban, G. M.; Zhou, J.; Asmis, K. R.; Neumark, D. M.; Gerber, R. B. *J. Chem. Phys.* **2007**, 127, 094305.

- (21) Wang, X. B.; Woo, H. K.; Kiran, B.; Wang, L. S. *Angew. Chem., Int. Ed.* **2005**, *44*, 4968.
- (22) Wang, X. B.; Woo, H. K.; Wang, L. S. *J. Chem. Phys.* **2005**, *123*, 051106.
- (23) Wang, X. B.; Yang, J.; Wang, L. S. *J. Phys. Chem. A* **2008**, *112*, 172.
- (24) Wang, X. B.; Wang, L. S. *Rev. Sci. Instrum.* **2008**, *79*, 073108.
- (25) Wang, X. B.; Xing, X. P.; Wang, L. S. *J. Phys. Chem. A* **2008**, *112*, 13271.
- (26) Vosko, S. H.; Wilk, L.; Nusair, M. *Can. J. Phys.* **1980**, *58*, 1200.
- (27) Lee, C.; Yang, W.; Parr, R. G. *Phys. Rev. B* **1988**, *37*, 785.
- (28) Becke, A. D. *J. Chem. Phys.* **1993**, *98*, 5648.
- (29) Dunning, T. H. Jr. *J. Chem. Phys.* **1989**, *90*, 1007.
- (30) Cizek, J. *Adv. Chem. Phys.* **1969**, *14*, 35.
- (31) Knowles, P. J.; Hampel, C.; Werner, H.-J. *J. Chem. Phys.* **1993**, *99*, 5219.
- (32) Raghavachari, K.; Trucks, G. W.; Pople, J. A.; Head-Gordon, M. *Chem. Phys. Lett.* **1989**, *157*, 479.
- (33) McLean, A. D.; Chandler, G. S. *J. Chem. Phys.* **1980**, *72*, 5639.
- (34) Clark, T.; Chandrasekhar, J.; Spitznagel, G. W.; Schleyer, P. v. R. *J. Comput. Chem.* **1983**, *4*, 294.
- (35) Frisch, M. J.; Pople, J. A.; Binkley, J. S. *J. Chem. Phys.* **1984**, *80*, 3265.
- (36) Head-Gordon, M.; Pople, J. A.; Frisch, M. J. *Chem. Phys. Lett.* **1988**, *153*, 503.
- (37) Saebo, S.; Almlöf, J. *Chem. Phys. Lett.* **1989**, *154*, 83.
- (38) Godbout, N.; Salahub, D. R.; Andzelm, J.; Wimmer, E. *Can. J. Chem.* **1992**, *70*, 560.
- (39) Gaussian 03, Revision C.02; Frisch, M. J.; et al.; Gaussian, Inc.: Wallingford CT, 2004.
- (40) MOLDEN 3.4 Schaftenaar, G. MOLDEN3.4, CAOS/CAMM Center, The Netherlands, 1998.
- (41) (a) Wang, X. B.; Ding, C. F.; Wang, L. S. *Phys. Rev. Lett.* **1998**, *81*, 3351. (b) Wang, L. S.; Ding, C. F.; Wang, X. B.; Nicholas, J. B. *Phys. Rev. Lett.* **1998**, *81*, 2667.
- (42) Wang, X. B.; Wang, L. S. *Nature (London)* **1999**, *400*, 245.
- (43) Wang, L. S.; Wang, X. B. *J. Phys. Chem. A* **2000**, *104*, 1978.
- (44) Wang, X. B.; Woo, H. K.; Wang, L. S.; Minofar, B.; Jungwirth, P. *J. Phys. Chem. A* **2006**, *110*, 5047.
- (45) Waters, T.; Woo, H. K.; Wang, X. B.; Wang, L. S. *J. Am. Chem. Soc.* **2006**, *128*, 4282.
- (46) Wang, X. B.; Woo, H. K.; Yang, J.; Kappes, M. M.; Wang, L. S. *J. Phys. Chem. C* **2007**, *111*, 17684.
- (47) Wang, X. B.; Matheis, K.; Ioffe, I. N.; Goryunkov, A. A.; Yang, J.; Kappes, M. M.; Wang, L. S. *J. Chem. Phys.* **2008**, *128*, 114307.

JP900682G